

Designing and Manufacturing the Multiple Jets Simulator and Experimental Investigation of the Multiple Jets in Crossflow

Saeed Toolani^{1*}, Mohamad Hojaji¹

¹Department of Mechanical Engineering, Najafabad Branch, Islamic Azad University, Najafabad, Iran

*Email of Corresponding Author: Saeed.toolani@gmail.com

Received: January 2, 2015; Accepted: February 16, 2015

Abstract

Designing and manufacturing the multiple jets simulator and experimental investigation of the multiple jets in crossflow at low velocity ratios have been studied Together with design and build a low-speed wind tunnel. A specific rake is used to determine the flow field pressure and changes in static pressure measured by pressure taps in the near field of the jets. There are generally three regions on the pressure distributions whose details depend on the velocity ratio. Study the flow field and surface pressure distribution at low velocity ratios shows that by the increase the velocity ratio, the total pressure of the jet stream decreases sharply. The effects of increasing the number of jet injection nozzles showed that the influence on the jet stream in the vertical plane is significant. However, the influence of Normal multiple jets on the plate is reduced. It also increases the number of nozzles reduced the pressure coefficient rather than the single-jet injection.

Keywords

Counter rotating vortex pair, Jet in crossflow, Jet simulator, Wake, Wind tunnel, Velocity ratio.

1. Introduction and Applications

Jet in crossflow which is widely investigated in theoretical, experimental and numerical studies is significantly related to engineering systems and modern technologies. Wide range of applications results from fifty years of experiments, researches and investigations in this field [1, 2]. Control of exhaust gas emitted from an industrial chimney is perhaps the simplest application of a jet in cross flow. Some of the applications of this phenomenon include the following [3]: control of industrial sewage to reduce the concentration of thermal and chemical pollution at the time of flowing into rivers, film cooling to reduce the surface temperature of gas turbine blades and petrochemical industries and refineries. Moreover, interaction of jet in cross flow has numerous applications in aviation and defense industries. Navigation and control of rockets, cruise and ballistic missiles, cooling the surface of the nose of multi-target missiles using cooled jets [4, 5], control the combustion process to optimize fuel and energy consumption in combustion engines such as scram jets [6] are also other applications of this phenomenon [7].

2. Flow Physics

Study of the jet in cross flow is important to get a better understanding and obtain maximum control of the flow field caused by this interaction. When a jet is injected normally in crossflow, fully complicated flow field will be created. The vertical structures are the main structures which contain the flow field, are known as horseshoe vortices (HSV), counter rotating vortices (CRV) and wake vortices (WV). Figure 1 shows the vertical structures due to injection of jet into cross flow.

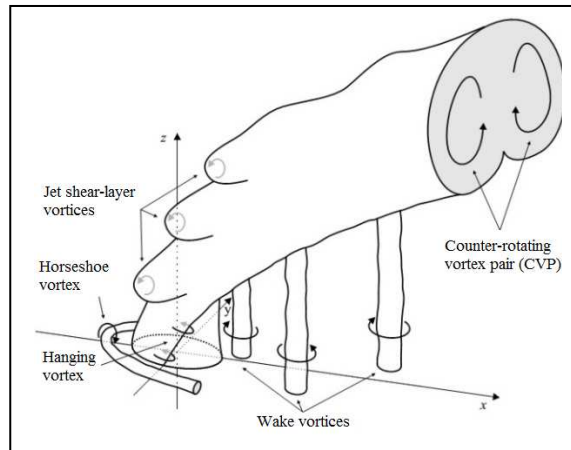


Figure1. Schematic interaction of jet with cross flow

Many studies have been made about the interaction of the jet with cross flow (JICF). Holdeman *et al.* [8] Studied the interference caused by multiple jets and subsonic cross flow. In this study, several nozzles were arranged at different intervals and in different layouts. The nozzles had different cross sections (such as circular and elliptical cross sections) and were used to study the effects of momentum flux. The findings of this study suggest that according to equation (1) a uniform flow distribution is obtained regardless of the diameter of nozzle cross sections. Moreover, convergence of nozzle walls also improves the composition of the jet and fluid flows.

$$1/L = \sqrt{J} \quad (1)$$

In the symmetrical arrangement of nozzles, the effect of the shape of the nozzle cross section is only evident in the near field of the jets. The flow permeability and combination with jets with an angle of 45 degrees are lower than those of jets arranged in one line.

Camussi *et al.* [9] studied interference of a jet in free stream with a very low Reynolds number ($Re < 100$). Vortex flow around the nozzle and the centerline of the jet were studied in the $1.5 < r \leq 4.5$ interval. Results show that jet Reynolds number plays a substantial role in flow instability and contributes to the formation of vortices.

Megerian *et al.* [10] studied the stability of the shear layer vortices caused by the interaction of a transverse jet and free stream at high Reynolds numbers and in the range of velocity ratio of $1 < r \leq 10$. In this research, an elevated nozzle and a nozzle at the wall level were employed. Velocity ratio variation was an important factor in the stability of the vortices of shear layers. The interaction of the jet and free stream at higher velocity ratios ($3.5 < r$) lead to the formation of unstable vortices. In the velocity ratio of $1.25 < r \leq 3.5$ the elevated and level jets show different behaviors.

Gautier *et al.* [11] studied the structure of counter rotating vortex pairs created by a jet with a circular cross section at lower velocity ratios ($r < 3$) in a water tunnel. In this study, the effects of jet velocity (V_j), free stream velocity (V_∞) and boundary layer thickness (δ) at low velocity ratio on vertical structure was studied. Results showed that variations of the velocity ratio can lead to changes in the thickness of the boundary layer.

According to the results of previous researches, it can be said that there is a scientific gap in the knowledge about multiple jets injected at low velocity ratios. In this study, the flow field resulting

from multiple jets in subsonic crossflow at low velocity ratios is studied. The air fluid was injected into the free stream at a specific pressure and velocity and its effects on the flow field was studied. To this end, three nozzles with a diameter of (D) were laid in a triangular arrangement on a flat plate (Figure2).

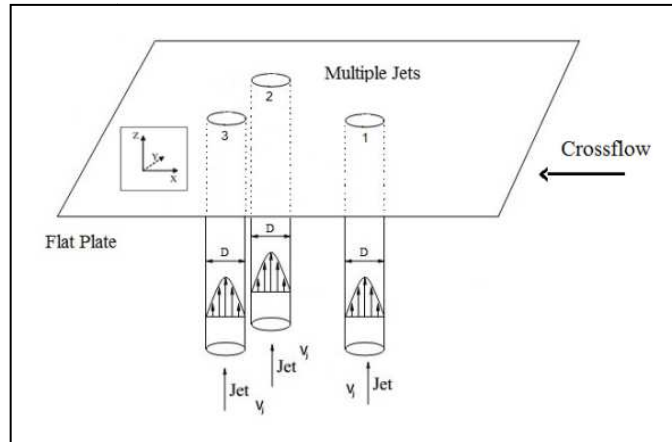


Figure2. Schematic of flat plate and multiple jets Injection nozzles

3. Experimental Apparatus

The objective of this study was to carry out an experimental study on the interference of the multiple jets in crossflow. To this end, a wind tunnel was designed and built. Also, in order to measure the quantities of concern, the required equipment was designed and built.

3.1 Design and Construction of the Wind Tunnel

The wind tunnel has been used in many research fields because of its vast research functions. Analysis of the details of flow fields around flight systems, vehicles and even towers is one of the main applications of wind tunnels. The first step to the design of a wind tunnel is to determine the size, shape and velocity of fluid flow in the test section [12,13]. The wind tunnel designed in this research is an open circuit low-speed and in draft tunnel. The tunnel has a square cross section built in a size of 0.45×0.45 (m^2). The tunnel has an approximate length of 8 (m) and the maximum velocity of the free stream in the test section is about 20 (m/s). At the beginning of the wind tunnel, where the fluid flows into the tunnel, a set of screens is used to reduce the fluid flow turbulent intensity. The converging nozzle which carries the fluid flow into the test chamber is connected to the front end of the test section chamber. The end of the test chamber is also connected to a diffuser. At the end of the wind tunnel an axial fan with a blade diameter of 0.8 m and maximum rotation frequency of 1730 RPM is installed. Moreover, the frequency of rotation of the axial fan was regulated by an inverter in order to control the free flow velocity in the test chamber (Figure 3).

Table shows the specifications of the built wind tunnel for this research.



Figure3. View of wind tunnel

Table1. Wind tunnel specification

N.O	length(m)	width(m)	height(m)
Test Section	1.2	0.45	0.45
Nozzle	1	1.27- 0.45	1.27- 0.45
Diffuser	3	0.8- 0.45	0.8- 0.45
Settling chamber	0.8	1.27	1.27

3.2 Assessment of Flow Quality in the Test Chamber

In order to calculate the free flow velocity in the test chamber, the static pressure of air flow was measured in different parts of the chamber using a Pitot tube. Figure 4 shows the distribution of velocity in the test chamber at different frequencies of rotation of the fan in the wind tunnel. According to this figure, the highest variations in the test section are about 7%. However, the variations were about 2.5% in maximum speed of the wind tunnel. Moreover, variations of velocity from the upstream to the downstream (nozzle to diffuser) are shown in Figure 5 using a number of pressure holes on the upper wall of the chamber. Similarly, the increase in the fan rotation frequency led to an increase in the velocity of free flow on the wall. An increase about 5% is observed in maximum velocity, which is due to the influence of the boundary layer thickness. In general, the comparison between Figures 4 and 5 shows the proper distribution of velocity in the test chamber.

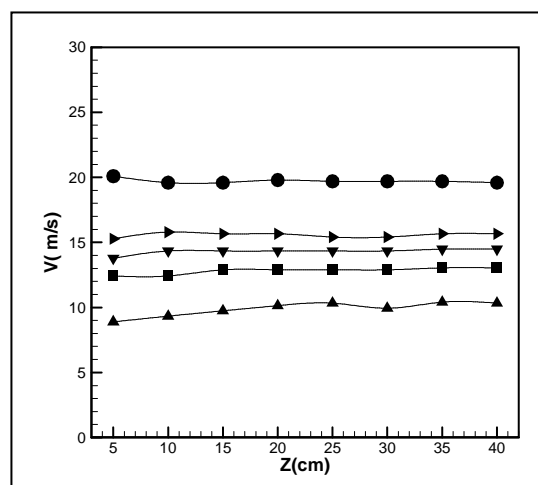


Figure4. Velocity distribution at cross section located 60 cm after the nozzle exit

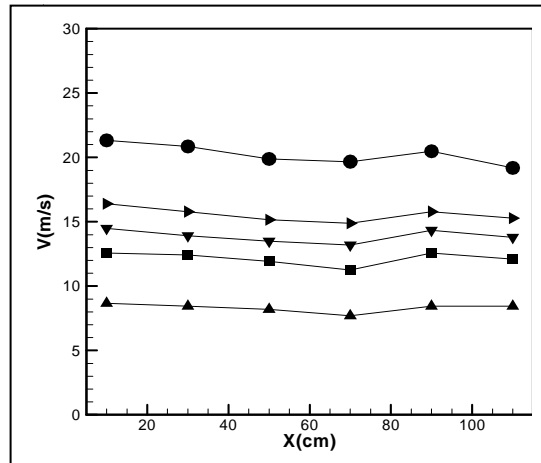


Figure5. Velocity distribution along the test section

3.3 Rake of Pitot Tubes

In order to study the flow field resulted from the interference of multiple jets and the free flow, a rake equipped with 22 pitot tubes was used. For analyzing the data measured by this instrument, it is possible to study variations of the total pressure in the flow field. The main frame of the rake is steel and steel tubes with an inner diameter of 1 mm are installed with 10 mm intervals on the rake. The rake is connected to manometer tubes using fully sealed special hoses (Figure 6). The rake can be moved using a traversing system in the wind tunnel and is fixed in certain stations depending on the type and significance of the test (Figure 7).

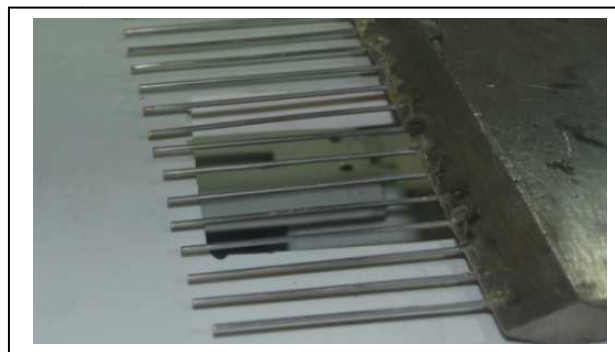


Figure6. Picture of rake

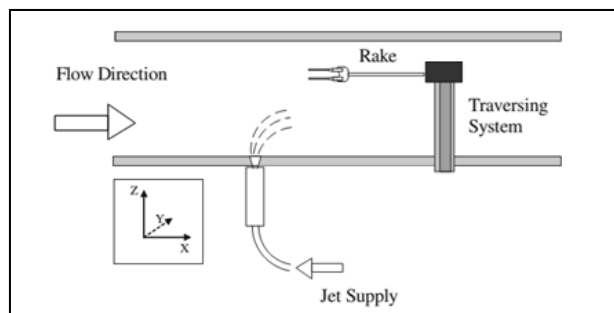


Figure7. Schematic of traversing system in the test section

4. Multiple Jets Simulation System

Triple jets are injected from nozzles beneath a flat plate in the test chamber. The flat plate was made of PVC and with dimensions $25.6 D \times 10D$ and a thickness of 10 mm. The front edge of the plate had a special shape to create a stable flow on the plate. In order to study the distribution of surface pressure, 249 pressure taps with an inner diameter of 1 mm were drilled downstream and upstream around the nozzles and along the center line. In order to simulate the interference of jet flow and free stream, three nozzles with an inner diameter of 25 mm (in a triangular arrangement) were created on the flat plate (Figure 8). The injection nozzles were made of polyethylene and were of equal heights. The jet stream was injected into a chamber from high-pressure air tanks through a pressure regulator. This cylindrical chamber was used to provide jets from triple nozzles at a constant velocity ratio. Moreover, in order to generate a flow with uniform discharge, three flow outputs with an angle of 120° were built on the chamber (Figure 9).

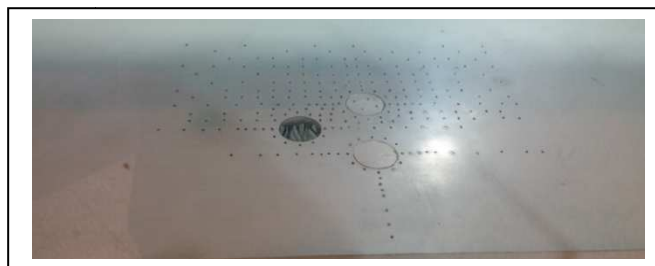


Figure8. Location of the nozzle on the flat plate

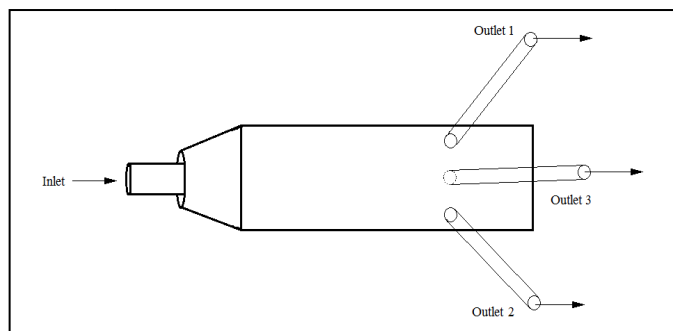


Figure9. Schematic of injection system

5. Results and Discussion

The effects of the interference between jets and free flow as well as distribution of pressure on a flat plate by pressure coefficient contours (C_p) at three velocity ratios were examined. In addition, the aforementioned flow field was also studied using the total pressure coefficient contours (C_{pt}) at three cross sections and two velocity ratios. Table 2 shows the flow properties.

Relations (1) and (2) were used respectively in order to show the surface pressure distribution and variations of the total pressure of the flow field. The first relation is the pressure coefficient and the second relation is a total pressure coefficient and q is the free stream dynamic pressure.

Table 2. Specifications of multiple jets and free stream

N.O	Jet (First Case)	Jet (Second Case)	Jet (Third Case)	Cross Flow
V (m/s)				17.3

ρ (kg/m ³)	1.2608	1.2608	1.2608	1.2032
	3.59×10^4	7.17×10^4	1.08×10^5	2.86×10^4
μ (kg/m.s)	1.7576×10^{-5}	1.7576×10^{-5}	1.7576×10^{-5}	1.826×10^{-5}
	1.16	2.31	3.47	----

$$C_p = \frac{P - P_\infty}{q} \tag{2}$$

$$C_{pt} = \frac{P_t - P_{t\infty}}{q} \tag{3}$$

$$q = \frac{1}{2} \rho_\infty V_\infty^2 \tag{4}$$

In order to assess the validity of the results, a comparison was made between the results of this study and reference [14]. In this research, the distribution of pressure caused by the discharge of a circular jet on a flat plate was studied. Table3 shows the test conditions of reference [14]. Figure 10 also depicts the results of the comparison between distribution of surface pressure on a flat plane near the nozzle and along the center line of the jet. At the downstream, with an increase in the distance from the jet injection nozzle and by an appropriate approximation, the pressure coefficient complies with the results. Moreover, a similar behavior is observed in the upstream. The results of this comparison indicate that the resulting pressure coefficients are satisfactory.

Table3. Comparison of flow specifications

N.O	Soullier	Present Study
V_∞ (m/s)	30	17.3
M	0.09	0.06
D(mm)	120	25
Flat Plate	21D × 21D	10D × 25.6D
Test Section	43D × 63D	18D × 48D
$Re_{c,f}$	24×10^4	2.86×10^4
r	2	2.31

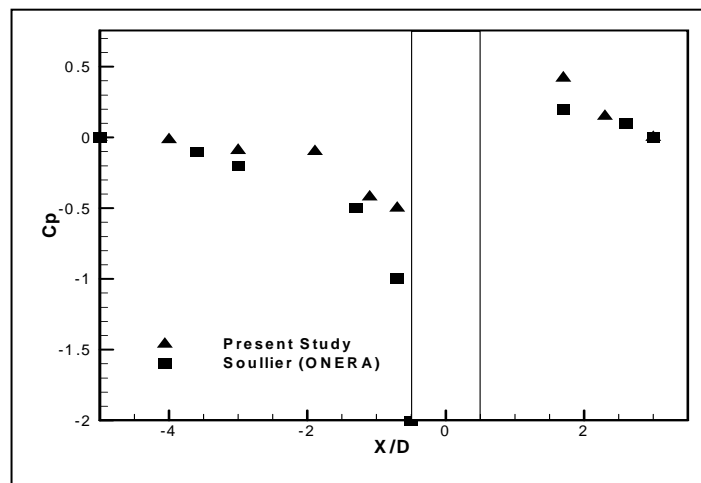


Figure10. Pressure distribution along the center line

5.1 Effect of Velocity Ratio on Distribution of Surface Pressure Around the Jet

Figure 11 shows the contours of pressure distribution around the nozzle exit. According to this figure the pressure coefficient has changed in the upstream, around the nozzle and in the downstream. In the upstream, the interaction between jets and crossflow led to the formation of flows with a positive pressure coefficient. The pressure coefficient is negative around the nozzles while the jet flow's accelerated near the nozzle and it leads to a reduction in the pressure coefficient. In the downstream, pressure approaches zero with an increase in the distance from the nozzles.

The distribution of the surface pressure caused by multiple jets at the velocity ratio of $r=1.16$ is depicted in Figure 12. Figure 13 and Figure 14 also, demonstrate the variations of pressure coefficient at velocity ratios $r=2.31$ and $r=3.47$. The area of the wake grows with an increase in the velocity ratio. However, the pressure coefficient in this area declines which shows an increase in the power of the wake. The reduction in pressure coefficient in the upstream of the jet no. (1) is observed. The reduction in pressure can be considered one of the effects of the increase in velocity ratio.

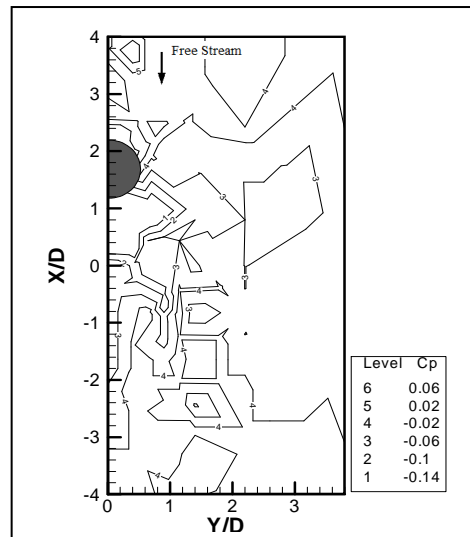


Figure11. Surface distribution around the nozzle exit ($r= 2.31$ - Single Jet Case)

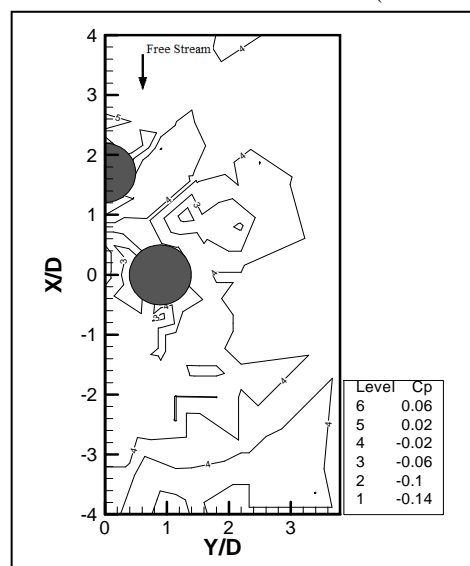


Figure12. Surface distribution around the nozzle exit ($r= 1.16$ - Multiple Jets Case)

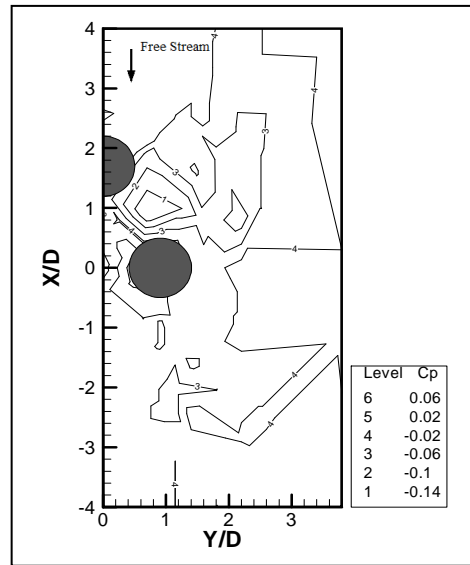


Figure13. Surface distribution around the nozzle exit ($r= 2.31$ - Multiple Jets Case)

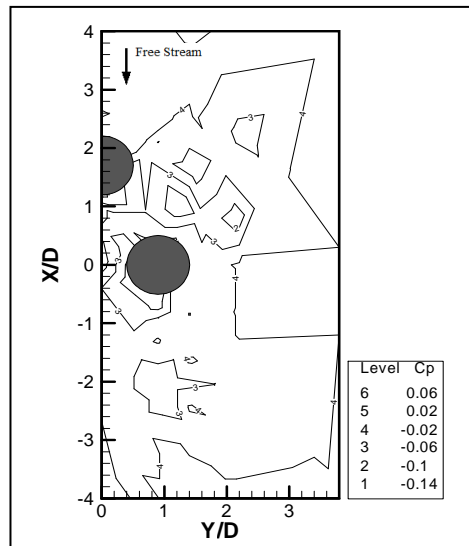


Figure14. Surface distribution around the nozzle exit ($r= 3.47$ - Multiple Jets Case)

5.2 Effects of Number of Exhausted Jets on the Flow Field

The interaction between the multiple jets and the free stream was examined by comparing the contours of total pressure coefficient at two cross sections. Table 4 presents the specifications of experiments carried out for this purpose. Contours of total pressure coefficient at the $X/D=4$ for single-jet and multiple jets in crossflow are shown in Figure15 and Figure16. The comparison between the contours of the total pressure coefficient indicates that an increase in the number of nozzles leads to a drastic decrease in the total pressure coefficient at this cross section. Moreover, the extent of flow penetration declines with an increase in the number of the nozzles at downstream of the nozzle exit. Figure17 depicts the flow field resulted from the single jet whereas Figure18 shows the same field resulted from multiple jets at the cross section $X/D=-8$. Similar to the previous section, in this part of the flat plate the increase in the number of nozzles leads to a drastic reduction in the total pressure coefficient.

The effects of the increase in the number of nozzles in four cross sections downstream of the nozzle exit are depicted in Figure19. The increase in the number of jets in the downstream at $X/D=-4$ leads to a 42.2% decline in the total pressure coefficient. It is worth nothing that the effect of the increase in the distance from the jet injection nozzle in the $X/D=-16$ section. As a result, the total pressure coefficient declines 69.2% in relation to the cross section $X/D=-4$ in the single jet state. In general, the increase in the number of nozzles causes a drastic decline in the total pressure coefficient.

Table4. Comparison of flow specifications

N.O	D(mm)	r	$R_{e_{c,f}}$
Single Jet	15	2 · 5	$1 · 982 \times 10^4$
Multiple Jets	25	2 · 31	$2 · 86 \times 10^4$

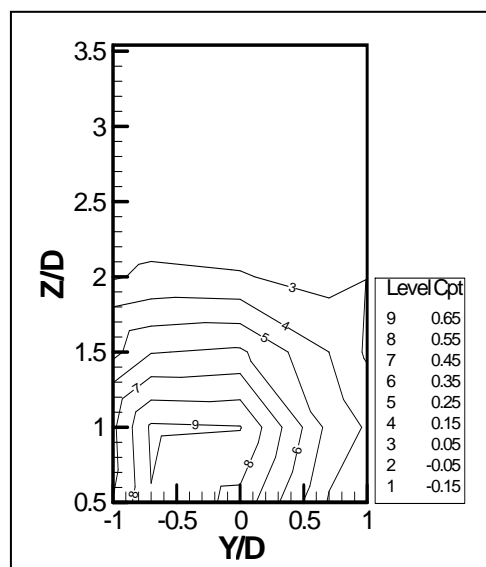


Figure15. Contours of total pressure at cross section $X/D=-4$ (Single Jet Case)

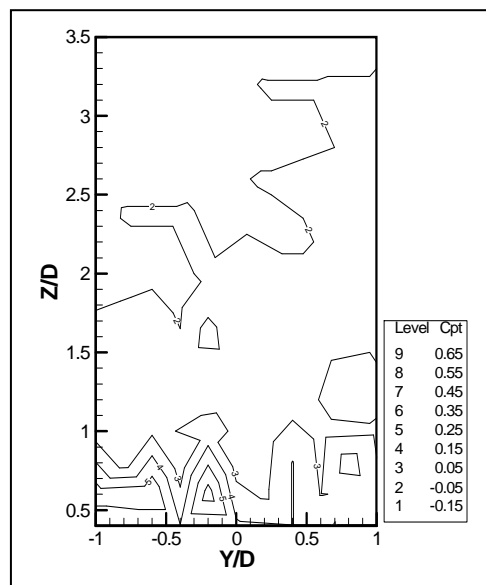


Figure16. Contours of total pressure at cross section $X/D=-4$ (Multiple Jets Case)

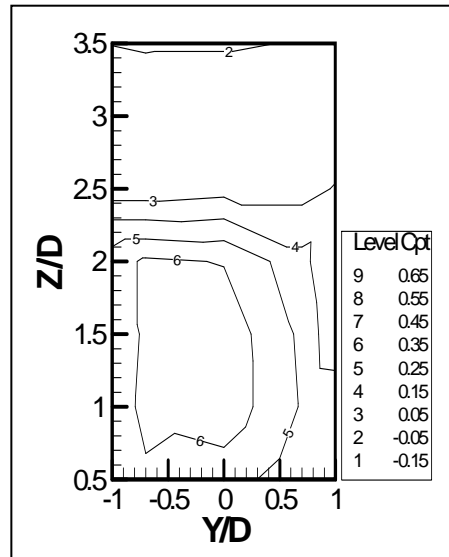


Figure17. Contours of total pressure at cross section $X/D=-8$ (Single Jet Case)

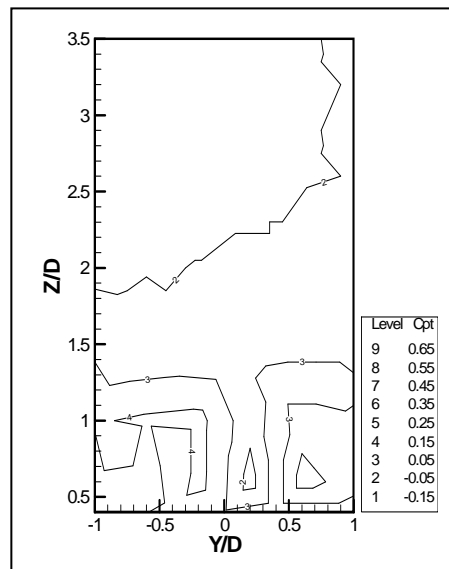


Figure18. Contours of total pressure at cross section $X/D=-4$ (Single Jet Case)

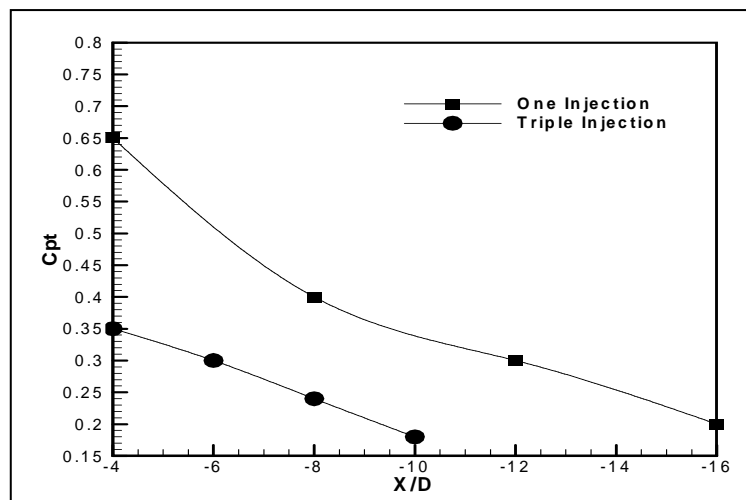


Figure19. Effect of number on the total pressure coefficient at downstream of the jet

5.3 Effects of Velocity Ratio on the Flow Field of Multiple Jets

The effects of interference between the multiple jets and the free stream at three velocity ratios and four cross sections downstream of the nozzle exit were also studied.

5.3.1 Flow Field at Velocity Ratio of $R=1.16$

The flow field resulted from the interference between the multiple jets and the free stream is shown in Figure 20. The aforementioned interference can be seen along the direction perpendicular to the flat plate until the $Z/D=2$. The plume resulted from the interference of the jet plume no. 2 is clearly seen. Flows resulted from jets no. 2 and 3 limit the interference between the jet no. (1) and the free stream. This effect influences the penetration of this flow over the width of the flat plate and along the vertical direction. The range of variations of the total pressure coefficient indicates that the coefficient declines with an increase in the distance from the flat plate and reaches $C_{pt}=0$ at sections higher than $Z/D=2$. The flow field shown in the $X/D=-4$ somewhat deviates from the center line of the triple jets. Seemingly, the angle between the axis of nozzles and the flat plate is deviated from the 90° slightly. However, previous research showed that the deviation of CVP from symmetry plane is observed at downstream of the nozzle exit [15].

Figure 21 and Figure 22 show the total pressure coefficient of the flow field in the crosssections $X/D=-6$ and $X/D=-8$. The drastic reduction in the total pressure coefficient is the effect of the increase in the distance from the jet exit. Moreover, the reduction in the total pressure coefficient of flow that flows from $Y/D=-1$ to $Y/D=0$ on the flat plate, can be clearly seen. Figure 23 shows the contour of the flow field of the cross section $X/D=-10$. As seen, the jet penetration did not grow significantly as compared to previous sections.

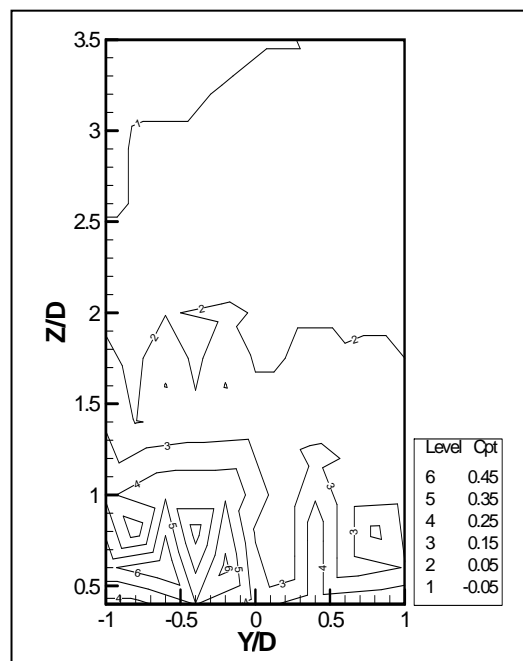


Figure 20. Contours of total pressure at cross section $X/D=-4$ ($r=1.16$)

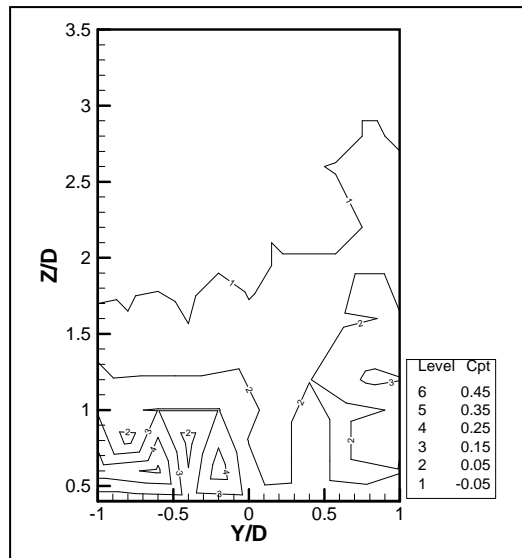


Figure21. Contours of total pressure at cross section $X/D=-6$ ($r=1.16$)

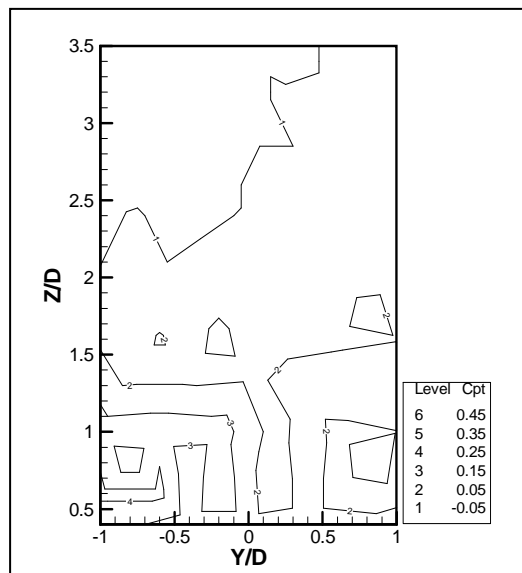


Figure22. Contours of total pressure at cross section $X/D=-8$ ($r=1.16$)

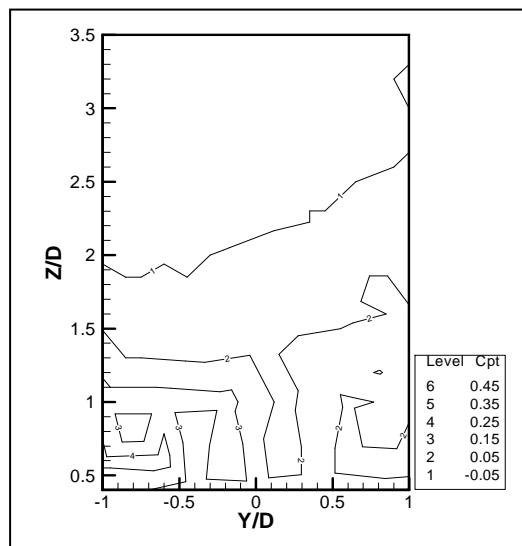


Figure23. Contours of total pressure at cross section $X/D=-10$ ($r=1.16$)

5.3.2 Flow Field at Velocity Ratio of $r=2.31$

Figure 24 shows the flow field resulted from the multiple jets at $X/D=-4$. As seen, the total pressure coefficient declined considerably as compared to the total pressure coefficient at the velocity ratio of $r=1.16$. However, the penetration of the jets declined drastically. Figure 25 to Figure 27 demonstrate variations of flow field at three different cross sections. The increase in the velocity ratio has led to the expansion of the multiple jets plume as compared to the previous state. Moreover, the total pressure coefficient also declines by increasing the distance from the nozzles.

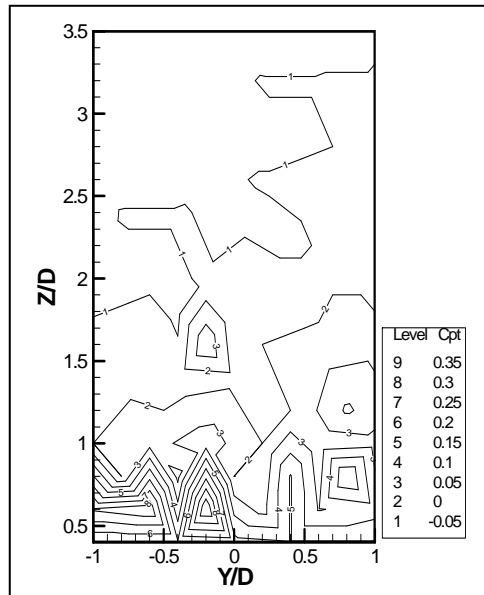


Figure24. Contours of total pressure at cross section $X/D=-4$ ($r=2.31$)

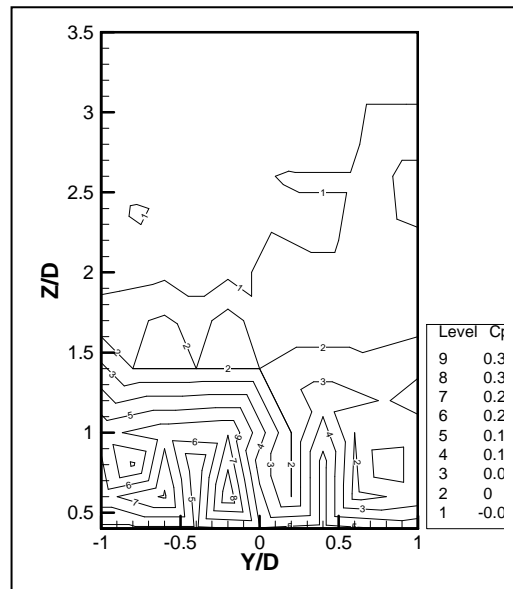


Figure25. Contours of total pressure at cross section $X/D=-6$ ($r=2.31$)

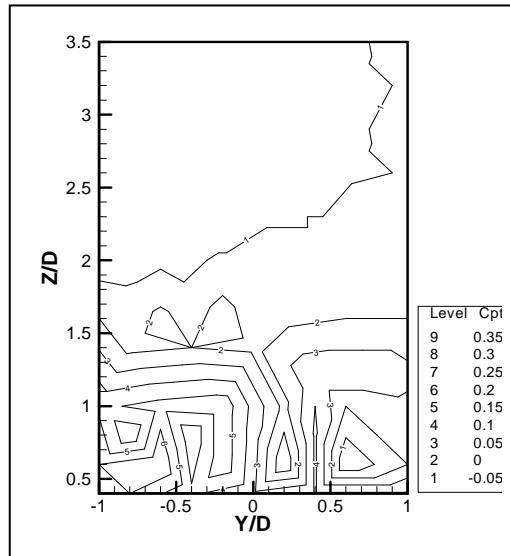


Figure26. Contours of total pressure at cross section X/D=-8 (r=2.31)

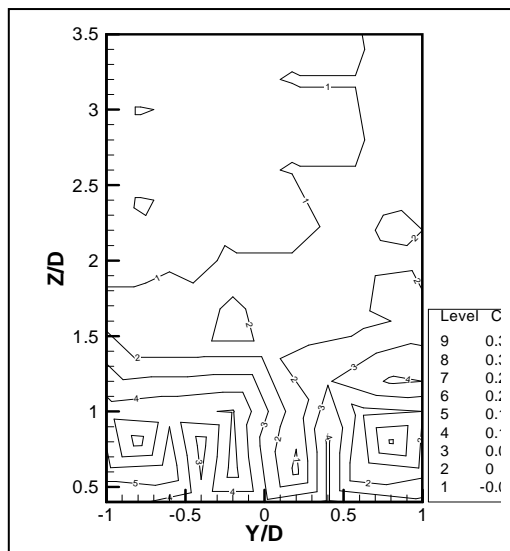


Figure27. Contours of total pressure at cross section X/D=-10 (r=2.31)

5.3.3 Flow Field at Velocity Ratio of r=3.47

Figure 28 shows the contours of the total pressure coefficient at X/D=-4 and r= 3.47. Comparison between contours of Figure 28 and similar sections at lower velocity ratios shows that the increase in the velocity ratio leads to a drastic reduction in the total pressure coefficient (Fig. 28). This descending trend is evidently shown in Figures 29, 30 and 31. Therefore, the velocity ratio leads to a reduction in the total pressure coefficient by increasing in the distance from the nozzles. The effects of the increased velocity ratio of the maximum total pressure coefficient are shown in Figure 32. The increase in the ratio of velocity from r=1.16 to r=2.31 leads to a decline in the maximum total pressure in downstream of the cross section X/D=-4. Moreover, the increase in the distance from the nozzle also reduces the intensity of this value at X/D=-8 and velocity ratio of r=1.16. Seemingly, the decrease in the total pressure coefficient of the jet mass at higher velocity ratios is caused by the higher interference between jets and the free stream. However, the above results show that the mixture of multiple jets at higher velocity ratios studied in this research is better because

although the total pressure of the jet mass increases at higher velocity ratios, it is lower in the flow field.

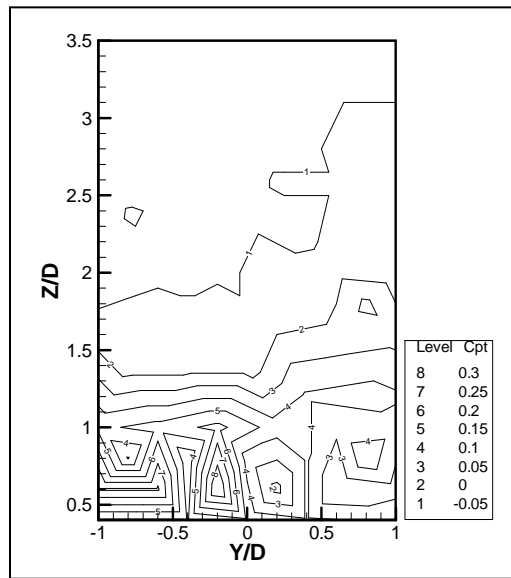


Figure28. Contours of total pressure at cross section X/D=-4 (r=3.47)

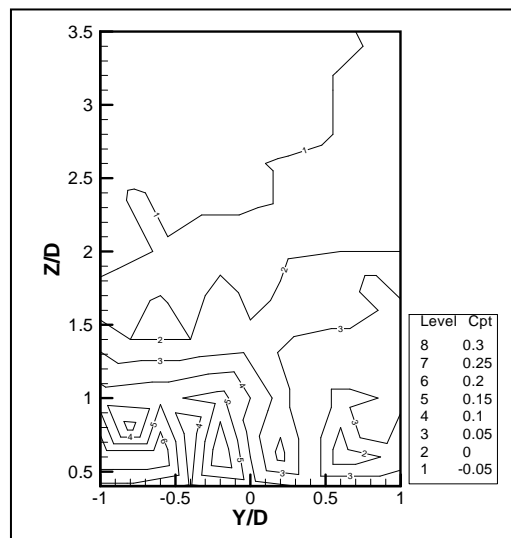


Figure29. Contours of total pressure at cross section X/D=-6 (r=3.47)

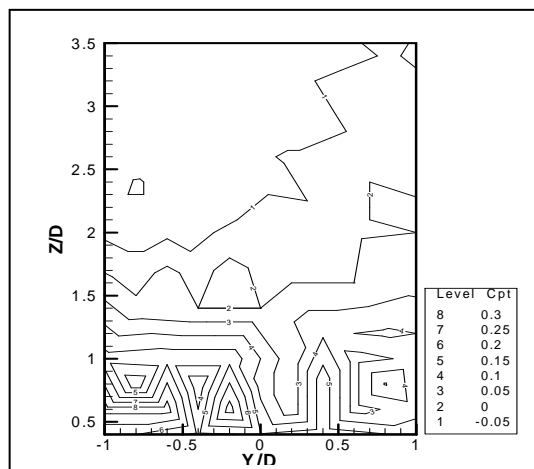


Figure30. Contours of total pressure at cross section X/D=-8 (r=3.47)

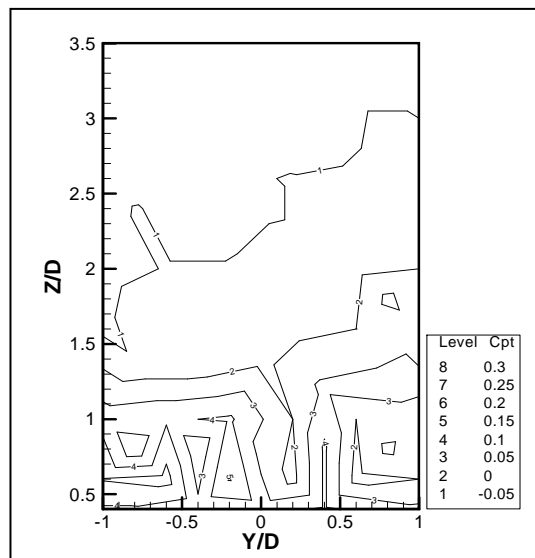


Figure31. Contours of total pressure at cross section X/D=-10 (r=3.47)

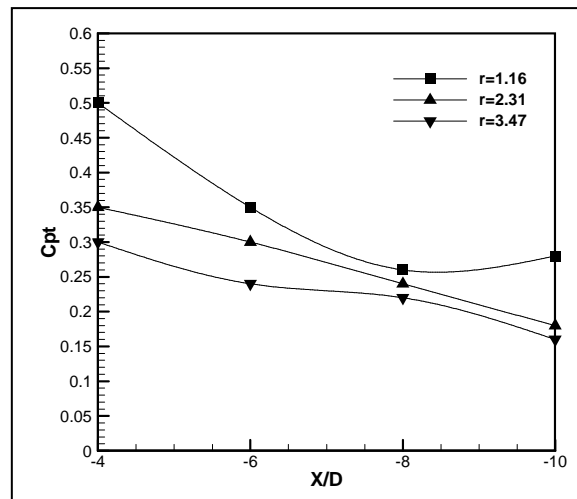


Figure32. Effect of velocity ratio of the maximum total pressure distribution at downstream of the jet

6. Conclusion

The objectives of this research included the following: design and construction of the jet simulator system and experimental study of the interference between multiple jets and a subsonic free stream. In this research, three jets in a triangular arrangement were used on the flat plate. The velocity of the free flow in all experiments was 17.3 (m/s). The ratio of jet velocity to free stream also varied between 1.16 and 3.47. A specific rake was used in order to measure the total pressure in the flow field. In addition, pressure holes were also drilled on the surface around the nozzle exit. Results showed that the triangular structure of the triple jets causes an increase in the areas influenced by the wake on the flat plate. However, as compared to the single jet case, the jet penetration along the direction perpendicular to the plate is reduced in the multiple jets case. The increase in the velocity ratio also led to the growth of the area and powered of the wake flow on the plate. Moreover, the surface pressure coefficient also declined through multiple jets injecting in the upstream with an increase in the velocity ratio. The increase in the distance from the jet injection nozzles also led to a reduction in the total pressure coefficient. However, the increase in the distance led to the expansion of the CVP along the perpendicular direction on the flat plate. Analysis of the effects of velocity

ratio on multiple jets flow fields showed that the growth of velocity ratio led to a drastic decrease in the total pressure coefficient and infuse a mixture of jets infused into free stream.

7. Nomenclature

X, Y, Z	Cartesian Coordinate (m)
q	Dynamic Pressure (Pa)
M	Mach Number
D	Nozzle Exit Diameter
p	Pressure (Pa)
C_p	Pressure Coefficient
Re	Reynolds Number
C_{pt}	Total Pressure Coefficient
v	Velocity (m/s)
r	Velocity Ratio

Greek letter

ρ	Density (kg/m ³)
μ	Viscosity (kg/m.s)

Subscript

∞	Free stream
j	Jet condition
t	Total condition

8. References

- [1] Margason, R. J. 1993. Fifty years of jet in cross flow research. *Progress in Energy and Combustion Science*, 15, 287–338.
- [2] Karagozian, A. R. 2010. Transverse jets and their control. *Progress in Energy and Combustion Science*, 36, 531-553.
- [3] Javadi. Kh., Taeibi-Rahni M. and Javadi A., 2004. New Approach to Control Turbulent Jet-into-CrossFlow Interaction- Skin Friction Drag Reduction. The 9th Fluid Dynamics Conf., Shiraz University, Shiraz,Iran.
- [4] Yusop, N. M., Ali, A. H., and Abdullah, M.Z. 2012. Computational Prediction into Staggered film Cooling Holes on Convex Surface of Turbine Blade. *International Communications in Heat and Mass Transfer*, 39, 1367–1374.
- [5] Bunker, R. S. 2005. A Review of Shaped Hole Turbine Film Cooling Technology. *Journal of Heat Transfer*, 127, 441-453.
- [6] Curran, E. T. 2001. Scramjet Engines: The First Forty Years. *Journal of Propulsion and Power*, 17, 1138-1148.
- [7] Chai, X. 2012. Numerical Simulations of High Speed Turbulent Jets in CrossFlow. University of Minnesota Digital Conservancy.

- [8] Holdeman, J. D. 1993. Mixing of Multiple Jets With A Confined Subsonic Crossflow. *Prog Energy Corabust. Sci*, 19, 31-70.
- [9] Camussi, R., Guj, G. and Stella, A. 2002. Experimental Study of A Jet in A Crossflow at Very Low Reynolds Number. *J. Fluid Mech*, 454, 113-144.
- [10] Megerian, S., Davitian, J., Alves, L. S. and Karagozian, A. R. 2007. Transverse-Jet Shear-Layer Instabilities. Part 1. Experimental studies. *J. Fluid Mech.*, 593, 93–129.
- [11] Cambonie, T., Gautier, N. and Aider, J. L. 2013. Experimental study of Counter-Rotating Vortex Pair Trajectories induced by a Round Jet in Cross-Flow at Low Velocity Ratios. *Experiments in Fluids*, 54(3), 1-13.
- [12] William, H., Rae, J. R. and Pope, A. 1984. *Low Speed Wind Tunnel Testing*. Wiley-Interscience., Second edition.
- [13] Pereira. J. D. 2010. *Wind Tunnels Aerodynamics, Models and Experiments*. Nova Science Publishers.
- [14] Soullier, A. 1972. Distribution of Pressure around the Jet Orifice, NASA Technical Translation. n. f-14066. Translation of "Essais a SI. MA Pour Recherches de Base Sur Les Interactions de Jet - Repartition des pressions autour de l' orifice du jet, Office National d' Etudes et de Recherches Aeronautiques , Chatillon, Document 1/253 GY, Part No. 1/5, April 1968, 97 pages.
- [15] Beresh, S. J., Henfling, J. F. and Erven, R. J. 2002. Surface Measurements of a Supersonic Jet in Subsonic Compressible Crossflow for the Validation of Computational Models. Sandia National Laboratories.

